Synlett S. Rengshausen et al. THIEME OPEN ACCESS Letter

Catalytic Hydrogenolysis of Substituted Diaryl Ethers by Using Ruthenium Nanoparticles on an Acidic Supported Ionic Liquid Phase (Ru@SILP-SO_3H)

Simon Rengshausen[a,b]
Fabian Etscheidt[b]
Johannes Großkurth[b]
Kylie L. Luska[b]
Alexis Bordet[a]
Walter Leitner*[a,b]

[a] Max-Planck-Institut für Chemische Energiekonversion, Stiftstraße 34-36, 45470 Mülheim an der Ruhr, Germany
[b] Institut für Technische und Makromolekulare Chemie, RWTH Aachen University, Worringerweg 2, 52074 Aachen, Germany
walter.leitner@cec.mpg.de

Published as part of the *30 Years SYNLETT – Pearl Anniversary Issue*

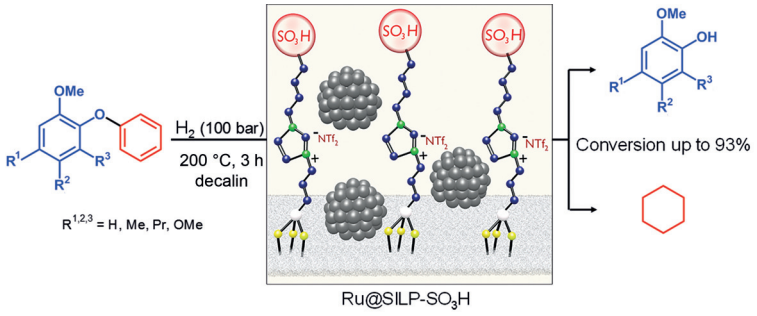

Received: 18.11.2018
Accepted after revision: 04.02.2019
Published online: 15.02.2019
DOI: 10.1055/s-0037-1611678; Art ID: st-2018-b0755-l

Abstract Catalytic hydrogenolysis of diaryl ethers is achieved by using ruthenium nanoparticles immobilized on an acidic supported ionic liquid phase (Ru@SILP-SO_3H) as a multifunctional catalyst. The catalyst components are assembled through a molecular approach ensuring synergistic action of the metal and acid functions. The resulting catalyst is highly active for the hydrogenolysis of various diaryl ethers. For symmetric substrates such as diphenyl ether, hydrogenolysis is followed by full hydrodeoxygenation producing the corresponding cycloalkanes as the main products. For unsymmetric substrates, the cleavage of the C–O bond is regioselective and occurs adjacent to the unsubstituted phenyl ring. As hydrogenation of benzene is faster than hydrodeoxygenation over the Ru@SILP-SO_3H catalyst, controlled mixtures of cyclohexane and substituted phenols are accessible with good selectivity. Application of Ru@SILP-SO_3H catalyst in continuous-flow hydrogenolysis of 2-methoxy-4-methylphenoxybenzene is demonstrated with use of commercial equipment.

Key words ruthenium nanoparticles, acidic SILP, multifunctional catalysis, diaryl ether cleavage, hydrogenolysis, deoxygenation, lignin

The catalytic reductive cleavage of C–O bonds in aryl ethers is an important transformation in synthetic organic chemistry, with possible applications including the synthesis of fine chemicals[1] and the production of fuels from biomass.[2] Breaking aromatic C–O bonds remains challenging, however, because of their high stability especially in diaryl ethers (bond dissociation energy = 82.5 kcal mol^{-1}).[3] As a result, significant efforts have been dedicated to the development of homogeneous[1c,4] and heterogeneous[5] catalysts for efficient hydrogenolysis of C–O linkages in diaryl ethers. Multifunctional catalytic systems are required to control the complex reaction network comprising the primary cleavage with parallel or secondary hydrogenation and deoxygenation processes (Scheme 1).

In the field of heterogeneous catalysis, third-row metal catalysts based on Ni,[5f,6] Co,[7] and Fe[8] were proved to be active for the hydrogenolysis of aromatic C–O bonds, providing high selectivities towards the production of aromatics and phenols. However, these catalysts typically possess limited activities and stabilities under the reaction conditions required for the transformation.[6b,7] Ru-based catalysts are also known to be highly active for the cleavage of aromatic C–O bonds, typically associated with hydrogenation of the aromatic moieties.[5e,9] Generally, the catalytically active materials for hydrogenolysis of diaryl ethers comprise a combination of metal and acid functionalities.[5g,9b,d,10] The bifunctional materials can lead to further hydrodeoxygenation of the primary aromatics produced to form

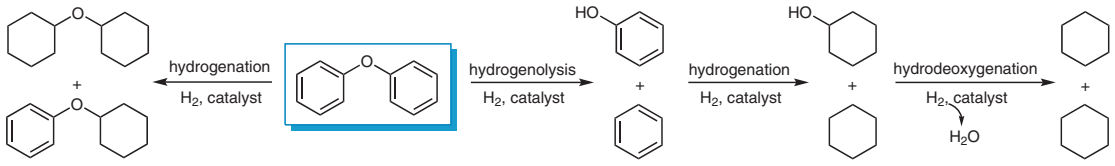

Scheme 1 Catalytic cleavage of diaryl ethers through hydrogenolysis and possible parallel and subsequent hydrogenation and hydrodeoxygenation, exemplified for diphenyl ether

completely saturated cycloalkanes.[11] To date, the influence of the substrate's substitution pattern on the product selectivity of the hydrogenolysis remains, however, fairly unexplored.[1c]

In the present work, ruthenium nanoparticles embedded in sulfonic acid-functionalized supported ionic liquid phases (Ru@SILP-SO_3H) are used as catalysts for the hydrogenolysis of substituted symmetric and unsymmetric diaryl ethers. A molecular approach to the preparation of bifunctional Ru@SILP-SO_3H catalysts was developed previously in our group and synergistic effects of the metal and acid components were demonstrated.[12] We now report that the materials are highly active for the hydrogenolysis of aromatic C–O bonds in various substrates, allowing controlled tandem integration with hydrodeoxygenation or hydrogenation of the resulting aromatic moieties. The substrate scope includes substitution patterns as found in lignin feedstock, and controlled mixtures of cyclohexane and phenol derivatives can be produced under continuous-flow operation.

The synthesis of Ru@SILP-SO_3H was achieved following a procedure previously reported by our group.[12a,b] In brief, the sulfonic acid-functionalized supported ionic liquid phase (SILP-SO_3H) was prepared through the condensation of the acidic ionic liquid [1-(4-sulfobutyl)-3-(3-triethoxysilyl-propyl)imidazolium]NTf_2 on dehydroxylated SiO_2 with a loading of 0.6 $mmol_{IL}$ g_{SiO2}^{-1}. The generation of ruthenium nanoparticles on the SILP-SO_3H phase involved the impregnation and in situ reduction of [Ru(2-methylallyl)$_2$(cod)] under an atmosphere of H_2 (100 bar) at 100 °C. A Ru loading of 0.27 wt% was determined by ICP, matching well the theoretical value of 0.32 wt%. TEM analysis of the resulting Ru@SILP-SO_3H material evidenced the formation of well-dispersed Ru NPs with a mean particle size of 1.7 ± 0.4 nm (Figure 1). Characterization details are summarized in Tables S1 and S2 in the Supporting Information.

The catalytic performance of Ru@SILP-SO_3H for the hydrogenolysis of diaryl ethers was assessed starting with diphenyl ether (**1**) as model substrate. According to the reaction network shown in Scheme 1, the catalytic transformation of **1** under hydrogen pressure can lead to the formation of several products, such as benzene (**1a**), phenol (**1b**), cyclohexane (**1c**), cyclohexanol (**1d**), and uncleaved mono- and disaturated ethers (**1e** and **1f**) (Table 1). Gratifyingly, the material proved very active leading to full conversion at a substrate/Ru loading of 500:1 under a standard set of reaction conditions [170 °C, H_2 (100 bar), 2 h; Table 1, entry 1]. Cyclohexane (**1c**) was obtained with a selectivity (S) of 62% indicating a significant contribution of hydrodeoxygenation from cyclohexanol (**1d**, S = 28%). The only observable side products were the saturated ethers **1e** + **1f** (S = 10%). Hydrogenolysis of dicyclohexyl ether (**1f**) under similar reaction conditions gave only 37% conversion, confirming that the main pathway for ether cleavage originates from the aromatic level (Table S3). Extending the reaction time for the conversion of **1** to 16 hours led to almost complete transformation into the fully saturated cyclic product **1c** (S = 94%; Table 1, entry 2).

Several control experiments were carried out in order to validate the synergistic action of the metal-acid functionalities of the supported material (Table 1, entry 3–7). The results show that the Ru-free acidic support SILP-SO_3H is not active for the cleavage of **1** under the reaction conditions considered, as expected (Table 1, entry 3). While the acid-free Ru@SILP is active for the hydrogenolysis of **1**, large amounts of saturated ethers (**1e** + **1f**) (S = 17%) are produced and cyclohexanol (**1d**) (S = 46%) is not efficiently deoxygenated to cyclohexane (**1c**) (S = 37%) (Table 1, entry 4). Employing a physical mixture of the two individual materials Ru@SILP and SILP-SO_3H resulted in only marginal improvement of the cleavage and deoxygenation activities (Table 1, entry 5). Use of a dispersion of Ru NPs in the nonsupported IL-SO_3H resulted in formation of **1c** as the major product, but the reaction reached only 34% conversion accompanied by agglomeration of the nanoparticles, in agreement with previous reports[12b] (Table 1, entry 6 and Figures S1, S2). The catalytic activity and selectivity of Ru@SiO_2 under these conditions were very low (Table 1, entry 7). Even after 16 hours the yield of the cleavage products could not

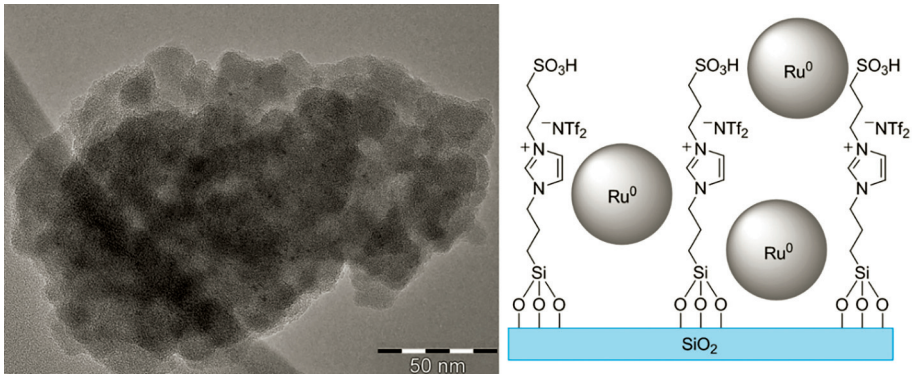

Figure 1 TEM micrograph of ruthenium nanoparticles embedded on acid-functionalized supported ionic liquid phase (Ru@SILP-SO_3H). The illustration on the right hand side is intended to indicate the close proximity of the metal and acid components, but does not reflect the actual size of the NPs.

Table 1 Hydrogenolysis of Diphenylether (**1**) with Use of Ru@SILP-SO_3H and Control Experiments[a]

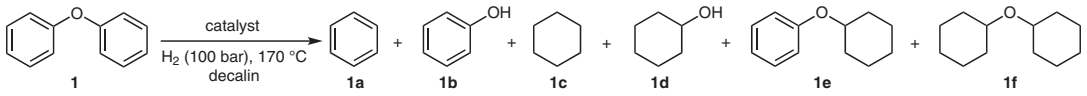

Entry	Catalyst	X (%)	Selectivity S (%)					
			1a	**1b**	**1c**	**1d**	**1e**	**1f**
1	Ru@SILP-SO_3H	>99	0	0	62	28	0	10
2[b]	Ru@SILP-SO_3H	>99	0	0	94	1	0	4
3	SILP-SO_3H	0	0	0	0	0	0	0
4[c]	Ru@SILP	>99	0	0	37	46	0	17
5	Ru@SILP + SILP-SO_3H	>99	0	0	46	33	0	21
6	Ru@IL-SO_3H	34	11	3	86	0	0	0
7	Ru@SiO_2	>99	0	0	17	18	0	65

[a] Ru@SILP-SO_3H (37.5 mg, 0.0012 mmol Ru), 2 h, 170 °C, H_2 (100 bar at rt), substrate (0.6 mmol, 500 equiv), decalin (0.5 mL).
[b] 16 h.
[c] Scale-up by factor 4. Conversion and selectivity determined by GC-FID by using hexadecane as an internal standard.

be further increased (Table S4). In addition, TEM analysis of Ru@SiO_2, Ru@SILP and Ru@SILP-SO_3H before and after catalysis (16 hours reaction time) evidenced severe aggregation in the case of Ru@SiO_2, whereas Ru@SILP and Ru@SILP-SO_3H were stable (Figure S3–S6). This demonstrates the importance of the ionic liquid layer in the SILP to stabilize the Ru NPs under these reaction conditions. Taken together, these results clearly demonstrate the synergistic bifunctional catalysis of metal and acid sites and the stabilizing effect of the IL moiety on the silica support.

To gain further insight into the influence of the substitution pattern at aromatic moieties for the hydrogenolysis with Ru@SILP-SO_3H, reactions of symmetric (Table 2) and unsymmetric (Table 3) diaryl ethers were performed under slightly adjusted reaction conditions (200 °C, 100 bar H_2, 3 h). Under these conditions, diphenyl ether (**1**) reacted nearly quantitatively to cyclohexane (**1c**) (S = 97%) through the hydrogenolysis/hydrodeoxygenation sequence, with only minor amounts of cyclohexanol (**1d**) (S = 1%) and benzene (**1a**) (S = 2%) as the side products (Table 2, entry 1). The presence of methyl groups in *para* position of the phenyl groups (4,4'-dimethyldiphenyl ether, **2**) did not affect the activity and selectivity of the catalyst, producing methylcyclohexane (**2c**) as sole product (S = 99%) (Table 2, entry 2). The introduction of methoxyl groups in *ortho* position (2,2'-dimethoxydiphenyl ether, **3**) also led to nearly full conversion of the substrate (96%). However, a mixture of products including aromatics [anisol (**3a**, S = 3%), guaiacol (**3b**, S = 12%)] and saturated compounds (**3c** + **3d** + **1c** + **1d**) was formed (Table 2, entry 3). These results indicate that the cleavage of the diaryl ether group was efficiently achieved, but the resulting aromatic monomers **3a** and **3b** were only partially hydrogenated to their saturated analogues **3c** and **3d**. This indicates the hindrance of the hydrogenation of the aromatic products by the methoxy substituents. In line with previous findings, the production of **1c** as the main product occurred through the hydrogenolysis of the methoxy group in **3c** and **3d** to form the corresponding alcohols and methane, followed by hydrodeoxygenation of the hydroxyl group.[12b]

On the basis of this observation, we further investigated the influence of the substitution pattern focusing on unsymmetric substrates possessing a methoxy group in *ortho* position. Several unsymmetric diaryl ethers were synthesized (see experimental procedures for details[13]) and subjected to hydrogenolysis by using Ru@SILP-SO_3H as catalyst under the previously established reaction conditions (Table 3). In all cases, cyclohexane was obtained as the major component together with phenols and their secondary products. The hydrogenolysis of the monosubstituted 2-methoxyphenoxybenzene (**4**) led to significant hydrodeoxygenation of the phenolic compounds, leading to overstoichiometric amounts of cyclohexane and only minor amounts of the aromatic products (Table 3, entry 1). The amount of aromatic products increased significantly to reach synthetically useful values for substrates **5** and **6**, which possess an additional methyl group in *meta* and *para* position, respectively (Table 3, entries 2 and 3). High conversions were achieved and the selectivities for creosol **5a** (37% selectivity, 41% isolated yield) and of iso-creosol **6a** (S = 42%) were nearly equivalent to those of cyclohexane. This trend continued for the sterically hindered substrates **7** and **8**, for which the substituted phenols **7a** and **8a** were obtained in high selectivities in an approximate 1:1 ratio with cyclohexane (Table 3, entries 4 and 5). Only small amounts of other possible side products were formed with these substrates.

Table 2 Hydrogenolysis of Symmetric Diaryl Ethers with Ru@SILP-SO_3H[a]

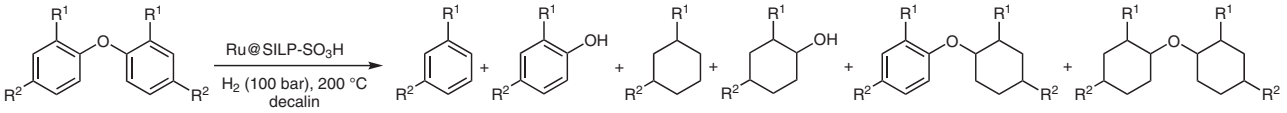

1: R^1 = H, R^2 = H
2: R^1 = H, R^2 = Me
3: R^1 = OMe, R^2 = H

Entry	Substrate	X (%)	Selectivity S (%)						
1	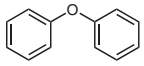 **1**	98	 **1a** 2	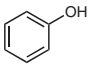 **1b** 0	 **1c** 97	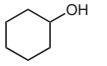 **1d** 1	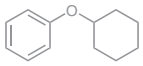 **1e** 0	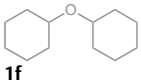 **1f** 0	-
2	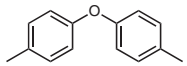 **2**	94	 **2a** 0	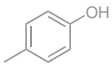 **2b** 0	 **2c** 99	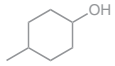 **2d** 0	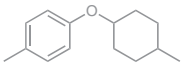 **2e** 0	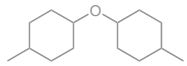 **2f** 0	-
3	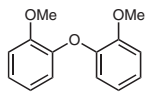 **3**	96	 **3a** 3	 **3b** 12	 **3c** 20	 **3d** 22	 **3e** 33	 **1d** 5	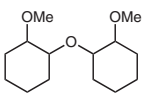 **3e** 5

[a] Ru@SILP-SO_3H (37.5 mg, 0.0012 mmol Ru), 3 h, 200 °C, H_2 (100 bar at rt), substrate (0.6 mmol, 500 equiv), decalin (0.5 mL). Conversion and selectivity determined by GC-FID with use of hexadecane as the internal standard.

Table 3 Hydrogenolysis of Unsymmetric Diaryl Ethers with Use of Ru@SILP-SO_3H[a]

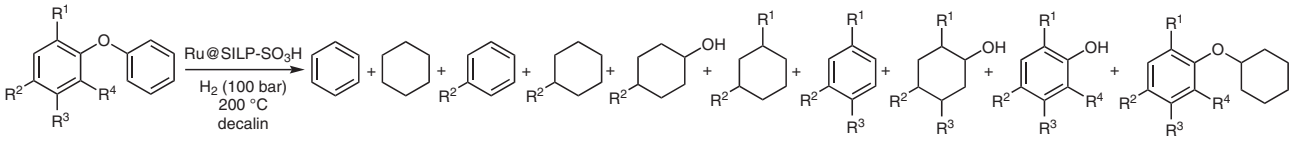

4: R^1 = OMe, $R^{2,3,4}$ = H
5: R^1 = OMe, R^2 = Me, $R^{3,4}$ = H
6: R^1 = OMe, R^3 = Me, $R^{2,4}$ = H
7: R^1 = OMe, R^2 = Pr, $R^{3,4}$ = H
8: $R^{1,4}$ = OMe, R^2 = Me, R^3 = H

Entry	Substrate	X (%)	Selectivity S (%)							
1	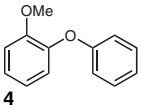 **4**	90	 **1a** 3	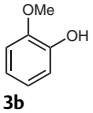 **3b** 21	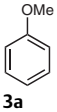 **3a** 3	 **1c** 62	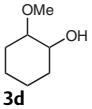 **3d** 7	 **1d** 1	 **3d** 3	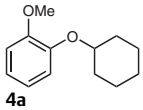 **4a** 1
2	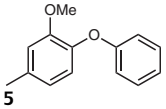 **5**	93	 **1a** 2	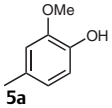 **5a** 37 (45%)[c]	 **2a** 1	 **1c** 46	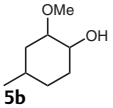 **5b** 1	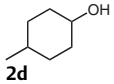 **2d** 3	**2c** 8	**5c** 1

Table 3 (continued)

Entry	Substrate	X (%)	Selectivity S (%)							
3	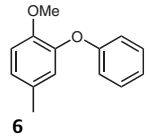 **6**	82	 **1a** 5	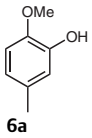 **6a** 42	 **2a** 1	 **1c** 43	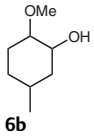 **6b** 1	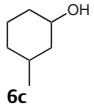 **6c** 2	 5	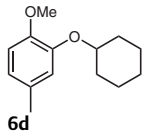 **2c** **6d** 1
4	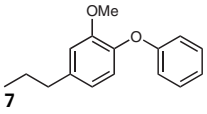 **7**	56	 **1a** 8	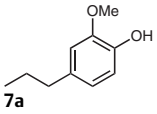 **7a** 40	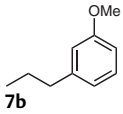 **7b** 2	 **1c** 48	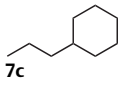 **7c** 3			
5[b]	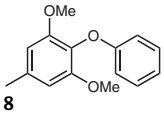 **8**	85	 **1a** 6	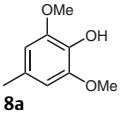 **8a** 47 (49%)[c]	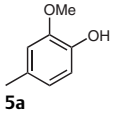 **5a** 1	 **1c** 45				

[a] Ru@SILP-SO_3H (37.5 mg, 0.0012 mmol Ru), 3 h, 200 °C, H_2 (100 bar at rt), substrate (0.6 mmol, 500 equiv), decalin (0.5 mL).
[b] Substrate (0.3 mmol, 250 equiv). Conversion and selectivity determined by GC-FID by using hexadecane as an internal standard.
[c] Isolated yield.

The selectivities shown in Table 3 provide valuable information on the reaction network of the sequential catalytic transformations. The initial hydrogenolysis of unsymmetric diaryl ethers can proceed in principle through two different routes, which are illustrated in Scheme 2. The production of cyclohexane and substituted phenols in comparable quantities strongly indicates that the ether cleavage occurs preferentially adjacent to the nonsubstituted arene ring with high regioselectivity (Scheme 2, Route 2).

After cleavage of the diaryl ethers, the Ru@SILP-SO_3H catalyst hydrogenates quickly the benzene produced to form cyclohexane. The substituted phenols are hydrogenated significantly slower, leaving the substituted phenols as the second main products. The conservation of the phenols' substituent pattern in the aromatic products is consistent with previous literature reports, which suggest that the defunctionalization of phenols requires, first, their hydrogenation to the corresponding substituted cyclohexanols.[12b]

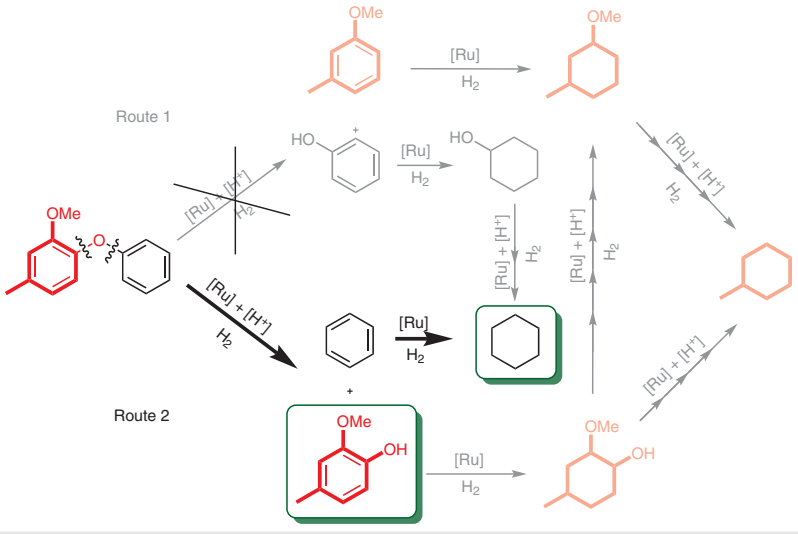

Scheme 2 Reaction pathway for the hydrogenolysis of unsymmetric diarylethers with use of Ru@SILP-SO_3H: example of 2-methoxy-4-methylphenoxybenzene

Once the hydrogenation occurs, subsequent hydrodeoxygenation reduces the oxygen content until, finally, the fully saturated cyclic products are obtained very slowly.

The hydrogenolysis of 2-methoxy-4-methylphenoxybenzene (**5**) by using the Ru@SILP-SO_3H catalyst was investigated under continuous-flow conditions in order to evaluate the product distribution as a function of time. In order to demonstrate the compatibility of the procedure with commercial equipment, the experiments were carried out in an H-Cube Pro™ equipped with a Phoenix Flow Reactor™ oven for high temperature experiments. After optimization of the reaction conditions towards high yields of creosol (**5a**), (Supporting Information, Tables S5–S7 for details), the performance of Ru@SILP-SO_3H was tested in a six hours run (Scheme 3). A temperature of 170 °C, a pressure of 40 bar H_2 (90 NmL min^{-1}), and a substrate flow of 0.3 mL min^{-1} were chosen corresponding to a residence time of τ = 12 s (see Supporting Information for further information). After an induction period (1–2 hours), the reaction reached a maximum conversion of 96% with good selectivity of creosol (**5a**) (34%) and alkanes (**1c** + **2c**) (43%), similar to what was obtained under batch conditions (Table 3, entry 2). In addition, small amounts of hydrogenated ethers (**5c**) (S = 11%), alcoholic intermediates (**1d** + **2d** + **5b**) (S = 8%) and benzene (**1a**) (S = 2%) were detected.

The conversion stayed within 86–96% for the period between two and six hours time on stream. ICP characterization of the catalyst after six hours on stream did not show any leaching of the Ru or the ionic liquid, and changes in the catalyst's textural properties were not detected by BET surface area analysis. Characterization of the catalyst before and after six hours on stream by using DRIFT-IR did not show any significant change in the regions corresponding to the characteristic absorption bands of the IL moiety (2900–3200 cm^{-1}: C–H stretches of the imidazolium ring and N-alkyl chain; 1450–1570 cm^{-1}: symmetric ring stretches of the imidazolium moieties; Supporting Information, Figures S7–9). In combination with the absence of leaching, this suggests that the ionic liquid layer is stable under the reaction conditions considered. In addition, the size and dispersion of the Ru NPs did not change during the reaction, as evidenced by TEM analysis (see Supporting Information, Tables S1, S2, and Figure S10 for characterization details). The Ru@SILP-SO_3H catalyst thus appears to be

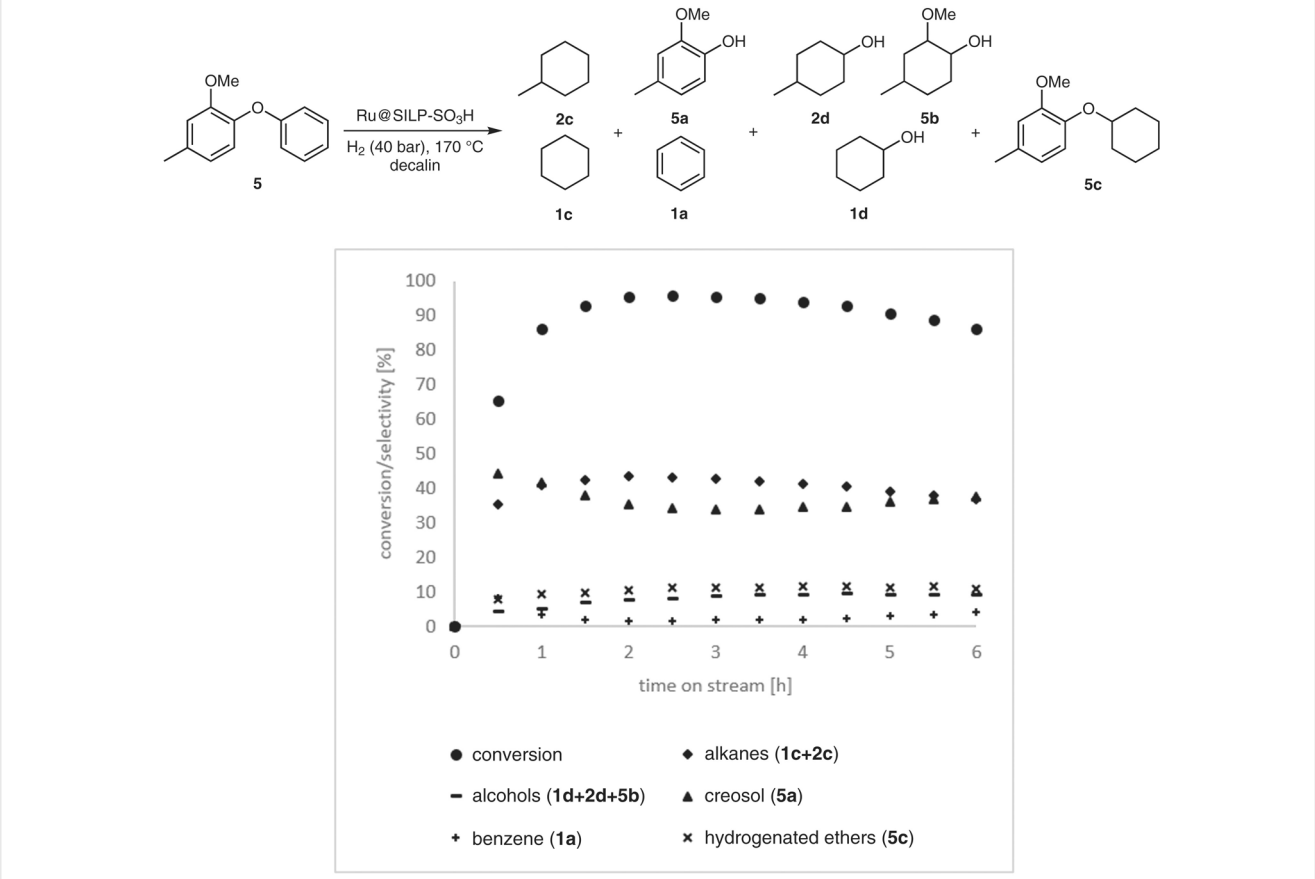

Scheme 3 Continuous flow hydrogenolysis of 2-methoxy-4-methylphenoxybenzene (**5**) by using Ru@SILP-SO_3H in an H-Cube™ reactor. Reaction conditions: Ru@SILP-SO_3H (439 mg, 0.014 mmol Ru), 0.3 mL min^{-1} substrate (0.025 mol L^{-1}), 90 NmL min^{-1} H_2 (40 bar), 170 °C, decalin. Conversion and selectivity were determined by GC-FID with use of hexadecane as an internal standard and based on the molar amount of the substrate used.

chemically stable under continuous flow conditions. Nevertheless, a small decrease in conversion and alkane yield after four hours suggests a loss of hydrogenolysis and hydrogenation activity with time. On the basis of previous findings, the loss of catalytic activity observed may be attributed to the accumulation of water on the catalyst during the reaction.[12b,14]

The hydrogenolysis of diaryl ethers was accomplished by using a bifunctional catalytic system consisting of ruthenium nanoparticles embedded on an acidic supported ionic liquid phase (Ru@SILP-SO_3H). The molecular design of the catalyst allowed for a close proximity between the metal and acid sites, which was shown to be a requirement for high catalytic activity. Various diaryl ethers with different substitution patterns were used as the substrates to study the catalytic activity and selectivity of Ru@SILP-SO_3H. While diphenyl ether and 4,4'-dimethyldiphenyl ether were readily converted to the corresponding cycloalkanes in high yields, the presence of methoxy groups as substituents hindered the hydrodeoxygenation of the cleaved moieties. In case of unsymmetric diaryl ethers, the cleavage of the C–O bond occurred adjacent to the unsubstituted phenyl ring regioselectively. This allows to achieve controlled formation of mixtures of methoxy-substituted phenols and cyclohexanes starting from substrates with substitution patterns as found in lignin-type feedstocks. Application of the Ru@SILP-SO_3H catalyst under continuous-flow conditions was demonstrated for the hydrogenolysis of 2-methoxy-4-methylphenoxybenzene. Production of a mixture of cyclohexane and creosol as the main products was achieved over six hours time on stream with conversions and yields similar to those observed under batch conditions. These results further substantiate the potential of molecular approaches for the design and the synthesis of multifunctional catalytic systems based on metal nanoparticles immobilized on functionalized supported ionic liquid phases (M@SILP-func) to control complex reaction networks involving consecutive and parallel hydrogenation and hydrogenolysis steps.

Funding Information

This work was supported by the Cluster of Excellence 'Tailor-Made Fuels from Biomass', which is funded under contract EXC 236 by the Excellence Initiative by the German federal and state governments to promote science and research at German universities.

Acknowledgment

The authors would like to acknowledge Cornelia Broicher (ITMC, RWTH Aachen) for BET absorption measurements, Hannelore Eschmann (ITMC, RWTH Aachen) and Elke Wilden (ITMC, RWTH Aachen) for GC measurements, and Wolfgang Falter (ITMC, RWTH Aachen) for GC-MS measurements. Furthermore, we would like to thank Norbert Pfänder and Adrian Schlüter (MPI für Kohlenforschung, Mülheim an der Ruhr) for TEM analysis.

Supporting Information

Supporting information for this article is available online at https://doi.org/10.1055/s-0037-1611678.

References and Notes

(1) (a) Cornella, J.; Zarate, C.; Martin, R. *Chem. Soc. Rev.* **2014**, *43*, 8081. (b) Bhatt, M. V.; Kulkarni, S. U. *Synthesis* **1983**, 249. (c) Sergeev, A. G.; Hartwig, J. F. *Science* **2011**, *332*, 439. (d) Samant, B. S.; Kabalka, G. W. *Chem. Commun.* **2012**, *48*, 8658.

(2) (a) Barta, K.; Ford, P. C. *Acc. Chem. Res.* **2014**, *47*, 1503. (b) Zhang, Z. R.; Song, J. L.; Han, B. X. *Chem. Rev.* **2017**, *117*, 6834. (c) Li, C. Z.; Zhao, X. C.; Wang, A. Q.; Huber, G. W.; Zhang, T. *Chem. Rev.* **2015**, *115*, 11559. (d) Zakzeski, J.; Bruijnincx, P. C.; Jongerius, A. L.; Weckhuysen, B. M. *Chem. Rev.* **2010**, *110*, 3552. (e) Xu, C. P.; Arancon, R. A. D.; Labidi, J.; Luque, R. *Chem. Soc. Rev.* **2014**, *43*, 7485. (f) Zaheer, M.; Kempe, R. *ACS Catal.* **2015**, *5*, 1675.

(3) (a) Dorrestijn, E.; Laarhoven, L. J. J.; Arends, I. W. C. E.; Mulder, P. *J. Anal. Appl. Pyrol.* **2000**, *54*, 153. (b) Parthasarathi, R.; Romero, R. A.; Redondo, A.; Gnanakaran, S. *J. Phys. Chem. Lett.* **2011**, *2*, 2660.

(4) (a) Nichols, J. M.; Bishop, L. M.; Bergman, R. G.; Ellman, J. A. *J. Am. Chem. Soc.* **2010**, *132*, 12554. (b) Kusumoto, S.; Nozaki, K. *Nat. Commun.* **2015**, *6*, 6296. (c) vom Stein, T.; Weigand, T.; Merkens, C.; Klankermayer, J.; Leitner, W. *ChemCatChem* **2013**, *5*, 439. (d) Deuss, P. J.; Scott, M.; Tran, F.; Westwood, N. J.; de Vries, J. G.; Barta, K. *J. Am. Chem. Soc.* **2015**, *137*, 7456. (e) Weickmann, D.; Plietker, B. *ChemCatChem* **2013**, *5*, 2170. (f) Saper, N. I.; Hartwig, J. F. *J. Am. Chem. Soc.* **2017**, *139*, 17667.

(5) (a) Van den Bosch, S.; Schutyser, W.; Vanholme, R.; Driessen, T.; Koelewijn, S. F.; Renders, T.; De Meester, B.; Huijgen, W. J. J.; Dehaen, W.; Courtin, C. M.; Lagrain, B.; Boerjan, W.; Sels, B. F. *Energ. Environ. Sci.* **2015**, *8*, 1748. (b) Cui, X. J.; Yuan, H. K.; Junge, K.; Topf, C.; Beller, M.; Shi, F. *Green Chem.* **2017**, *19*, 305. (c) Cao, Z.; Engelhardt, J.; Dierks, M.; Clough, M. T.; Wang, G.-H.; Heracleous, E.; Lappas, A.; Rinaldi, R.; Schüth, F. *Angew. Chem. Int. Ed.* **2017**, *56*, 2334. (d) Song, Q.; Wang, F.; Xu, J. *Chem. Commun.* **2012**, *48*, 7019. (e) Wu, H. R.; Song, J. L.; Xie, C.; Wu, C. Y.; Chen, C. J.; Han, B. X. *ACS Sustain. Chem. Eng.* **2018**, *6*, 2872. (f) He, J. Y.; Zhao, C.; Lercher, J. A. *J. Am. Chem. Soc.* **2012**, *134*, 20768. (g) Wang, X. Y.; Rinaldi, R. *Catal. Today* **2016**, *269*, 48. (h) Wang, M.; Shi, H.; Camaioni, D. M.; Lercher, J. A. *Angew. Chem. Int. Ed.* **2017**, *56*, 2110. (i) Chatterjee, M.; Ishizaka, T.; Suzuki, A.; Kawanami, H. *Chem. Commun.* **2013**, *49*, 4567.

(6) (a) van Duzee, E. M.; Adkins, H. *J. Am. Chem. Soc.* **1935**, *57*, 147. (b) Gao, F.; Webb, J. D.; Hartwig, J. F. *Angew. Chem. Int. Ed.* **2016**, *55*, 1474. (c) Sergeev, A. G.; Webb, J. D.; Hartwig, J. F. *J. Am. Chem. Soc.* **2012**, *134*, 20226. (d) He, J. Y.; Zhao, C.; Mei, D. H.; Lercher, J. A. *J. Catal.* **2014**, *309*, 280. (e) Zaheer, M.; Hermannsdorfer, J.; Kretschmer, W. P.; Motz, G.; Kempe, R. *ChemCatChem* **2014**, *6*, 91. (f) Zhang, J. G.; Teo, J.; Chen, X.; Asakura, H.; Tanaka, T.; Teramura, K.; Yan, N. *ACS Catal.* **2014**, *4*, 1574. (g) Zhang, J. G.; Asakura, H.; van Rijn, J.; Yang, J.; Duchesne, P.; Zhang, B.; Chen, X.; Zhang, P.; Saeys, M.; Yan, N. *Green Chem.* **2014**, *16*, 2432. (h) Wang, X.; Rinaldi, R. *ChemSusChem* **2012**, *5*, 1455.

(7) Ren, Y. L.; Tian, M.; Tian, X. Z.; Wang, Q.; Shang, H. T.; Wang, J. J.; Zhang, Z. C. *Catal. Commun.* **2014**, *52*, 36.
(8) Ren, Y.; Yan, M.; Wang, J.; Zhang, Z. C.; Yao, K. *Angew. Chem. Int. Ed.* **2013**, *52*, 12674.
(9) (a) Bulut, S.; Siankevich, S.; van Muyden, A. P.; Alexander, D. T. L.; Savoglidis, G.; Zhang, J. G.; Hatzimanikatis, V.; Yan, N.; Dyson, P. J. *Chem. Sci.* **2018**, *9*, 5530. (b) Wang, H.; Ruan, H.; Feng, M.; Qin, Y.; Job, H. M.; Luo, L.; Wang, C.; Engelhard, M. H.; Kuhn, E.; Chen, X.; Tucker, M. P.; Yang, B. *ChemSusChem* **2017**, 1846. (c) Huang, Y. B.; Yan, L.; Chen, M. Y.; Guo, Q. X.; Fu, Y. *Green Chem.* **2015**, *17*, 3010. (d) Zhang, W.; Chen, J. Z.; Liu, R. L.; Wang, S. P.; Chen, L. M.; Li, K. G. *ACS Sustain. Chem. Eng.* **2014**, *2*, 683.
(10) (a) Park, H. W.; Hong, U. G.; Lee, Y. J.; Song, I. K. *Catal. Commun.* **2012**, *20*, 89. (b) Jin, S. H.; Xiao, Z. H.; Chen, X.; Wang, L.; Guo, J.; Zhang, M.; Liang, C. H. *Ind. Eng. Chem. Res.* **2015**, *54*, 2302.
(11) (a) Zhao, C.; Lercher, J. A. *ChemCatChem* **2012**, *4*, 64. (b) Yan, N.; Yuan, Y. A.; Dykeman, R.; Kou, Y. A.; Dyson, P. J. *Angew. Chem. Int. Ed.* **2010**, *49*, 5549. (c) Wang, H. L.; Ruan, H.; Pei, H. S.; Wang, H. M.; Chen, X. W.; Tucker, M. P.; Cort, J. R.; Yang, B. *Green Chem.* **2015**, *17*, 5131. (d) Luo, Z. C.; Zheng, Z. X.; Wang, Y. C.; Sun, G.; Jiang, H.; Zhao, C. *Green Chem.* **2016**, *18*, 5845.
(12) (a) Luska, K. L.; Julis, J.; Stavitski, E.; Zakharov, D. N.; Adams, A.; Leitner, W. *Chem. Sci.* **2014**, *5*, 4895. (b) Luska, K. L.; Migowski, P.; El Sayed, S.; Leitner, W. *Angew. Chem. Int. Ed.* **2015**, *54*, 15750. (c) Luska, K. L.; Migowski, P.; El Sayed, S.; Leitner, W. *ACS Sustain. Chem. Eng.* **2016**, *4*, 6186. (d) Luska, K. L.; Migowski, P.; Leitner, W. *In Nanocatalysis in Ionic Liquids* 2016. (e) Offner-Marko, L.; Bordet, A.; Moos, G.; Tricard, S.; Rengshausen, S.; Chaudret, B.; Luska, K. L.; Leitner, W. *Angew. Chem. Int. Ed.* **2018**, *57*, 12721.
(13) **Experimental Procedures**
Safety warning: High-pressure experiments with compressed H_2 must be carried out only with appropriate equipment and under rigorous safety precautions.
General: If not otherwise stated, the syntheses of the ionic liquids (ILs), the supported ionic liquid phases (SILPs), and the nanoparticles immobilized on SILPs (Ru@SILP and Ru@SILP-SO_3H) were carried out under an inert atmosphere by using standard Schlenk techniques or inside a glovebox. After synthesis, ILs, SILPs, Ru@SILP, and Ru@SILP-SO_3H were stored under an inert atmosphere. If not otherwise stated solvents were used after distillation without any further purification. For reactions under an inert atmosphere, solvents were additionally dried with molecular sieves (4 Å) and degassed by flushing solvents with argon. For catalysis decalin (from ACROS, 99% anhydrous) was used without purification. The precursor [Ru(2-methylallyl)$_2$(cod)] was commercially available from Umicore. All other chemicals and solvents were purchased from commercial suppliers and used without purification.
Synthesis of catalysts: The Ru@SILP, Ru@SILP-SO_3H, and Ru@IL-SO_3H were synthesized as previously reported and Ru@SiO_2 was synthesized accordingly.[12a]
Synthesis of substrates: The synthesis of diarylethers was carried out as previously reported.[1c]A round-bottom Schlenk-flask (250 mL) was equipped with a magnetic stir bar, copper iodide (456 mg, 2.40 mmol, 10.0 mol%), picolinic acid (590 mg, 4.80 mmol, 20.0 mol%), and potassium phosphate (10.2 g, 48.0 mmol, 2.00 equiv). A second Schlenk flask (100 mL) was charged with the aryl iodide (24.0 mmol, 1 equiv), the phenol (28.8 mmol, 1.2 equiv), and anhydrous DMSO (50 mL). The solution of flask 2 was transferred into flask 1 under flowing Argon and the reaction mixture was stirred for 20 h at 100 °C, subsequently. After cooling down, the reaction mixture was diluted with a 1:1 mixture of a saturated aqueous solution of NH_4Cl (200 mL) and H_2O (200 mL). After extraction with CH_2Cl_2 (3 × 200 mL) the combined organic phases were washed with a 5% aqueous solution of KOH (300 mL) and brine (300 mL). After drying the mixture with Na_2SO_4 the solvent was removed and the crude reaction mixture was preadsorbed on silica gel. The purification of the crude mixture was achieved with use of silica gel. Remaining iodine compounds caused the deactivation of the catalyst in subsequent catalytic reactions and therefore had to be separated carefully. This afforded in some cases purification by two subsequent chromatography columns. Full characterization of all substrates can be found in the Supporting Information.
2,6-Dimethoxy-4-methylphenoxybenzene: Prepared according to the general procedure by using iodobenzene (5.00 g, 24.0 mmol) and 2,6-dimethoxy-4-methylphenol (4.8 g, 28.8 mmol). The crude product was purified by flash column chromatography (eluent: ethyl acetate/*n*-pentane 1:8). 2,6-Dimethoxy-4-methylphenoxybenzene was obtained as a slightly off-white solid (4.46 g, 18.3 mmol) in 76% yield. ^{1}H NMR (500 MHz, $CDCl_3$): δ = 7.29–7.26 (m, 2 H), 7.02–6.98 (m, 1 H), 6.93–6.90 (m, 2 H), 6.51 (s, 2 H), 3.79 (s, 6 H), 2.42 (s, 3 H) ppm. ^{13}C NMR (125.7 MHz, $CDCl_3$): δ = 158.77 (C), 153.23 (C), 135.65 (C), 129.84 (C), 129.39 (CH), 121.52 (CH), 114.87 (CH), 106.28 (CH), 56.33 (CH_3), 22.24 (CH_3) ppm. HRMS (EI): *m*/*z* 244.11.
Batch catalysis: In a typical experiment, Ru@SILP (37.5 mg, 0.0012 mmol Ru), substrate (0.6 mmol, 500 equiv), and decalin (0.5 mL) were combined in a glass insert and placed in a high-pressure autoclave. After purging the autoclave with H_2, the reaction mixture was stirred at 170 °C in an aluminium heating cone under 120 bar H_2 (pressurized at 100 bar H_2 at rt). After the reaction, the autoclave was cooled in an ice bath, carefully vented, and the reaction mixture filtered before GC analysis with use of hexadecane as an internal standard. In some cases a gap in mass balance was observed because of the loss of cyclohexane in the headspace of the autoclave (scale-up decreased this error).
Isolated yield (5a): The catalysis was scaled up by a factor of 5. After reaction the decalin phase was isolated and the catalyst washed with decalin (1 × 5 mL). The combined organic phases were extracted with aqueous KOH (3 × 10 mL, 0.3 M). The KOH phase was washed with *n*-pentane (3 × 10 mL) and neutralized with aqueous HCl, subsequently. After neutralization, the aqueous phase was extracted with CH_2Cl_2 (4 × 20 mL). After drying the CH_2Cl_2 phase with $MgSO_4$ and removal of the solvent a yellow-brownish oil (186 mg, 1.35 mmol) was obtained in 45% yield (See Supporting Information, Figure S11 for characterization).
Continuous flow catalysis: A 70 mm CatCart® ($V_{packed\ reactor}$ = 0.5126 mL) was filled with Ru@SILP-SO_3H (439 mg, 0,014 mmol Ru) and installed into the H-Cube Pro™. Prior to catalysis the catalyst was flushed with decalin (1 mL min^{-1} for 30 min). Then, the reactor was pressurized to 40 bar H_2 (90 NmL min^{-1}) and heated to 170 °C. When reaching stable reaction conditions, the substrate solution (0.025 M in decalin) was introduced into the system (0.3 mL min^{-1}). The reaction was allowed to equilibrate for 30 min before the first samples were collected. The reaction mixture was analysed by GC analysis with use of hexadecane as an internal standard.
(14) Mellmer, M. A.; Sener, C.; Gallo, J. M. R.; Luterbacher, J. S.; Alonso, D. M.; Dumesic, J. A. *Angew. Chem. Int. Ed.* **2014**, *53*, 11872.